J Nanopart Res (2019) 21:94
https://doi.org/10.1007/s11051-019-4511-8

RESEARCH PAPER

Effect of silica nanotubes on characteristic and performance of PVDF nanocomposite membrane for nitrate removal application

Hamideh Yari · Majid Pakizeh · Mahdieh Namvar-Mahboub

Received: 9 August 2018 / Accepted: 15 March 2019
© Springer Nature B.V. 2019

Abstract In this work, impact of synthesized silica nanotubes (SNTs) on morphology and performance of polyvinylidene fluoride (PVDF) nanocomposite membrane was studied. For this purpose, SNTs were synthesized using hydrothermal method, characterized by different techniques, and finally used as filler in nanocomposite membrane preparation. The PVDF/SNTs nanocomposite membranes were fabricated via phase inversion method at different dosage of SNTs (1–6 wt.%). As-prepared membranes and SNTs were characterized by attenuated total reflectance Fourier transform infrared (ATR-FTIR) spectroscopy, scanning electron microscopy (SEM), transmission electron microscopy (TEM), small-angle X-ray scattering (SAXS), and contact angle measurement. The results confirmed by incrementing SNTs dosage, hydrophilicity of PVDF membrane was increased. The effect of SNTs on the membrane performance was studied through nitrate removal at operating pressure of 7 bar. The results showed that the optimal performance parameters (nitrate rejection and pure water permeability (PWP) were obtained at SNTs dosage of 4%. The effect of feed concentration (50, 100, and 150 mg/L) on nitrate separation performance was also investigated and it was found that the maximum rejection of 86% and PWP of 11.58 (L/m^2.h.bar) were achieved for optimum PVDF/SNTs membrane at 150 mg/L. Finally, antifouling properties of optimum PVDF/SNTs membrane were investigated.

Keywords Silica nanotubes · Nitrate removal · Nanofiltration membrane · PVDF · Wastewater treatment · Nanofiltration · Environmental effects

H. Yari · M. Pakizeh (✉)
Department of Chemical Engineering, Faculty of Engineering, Ferdowsi University of Mashhad, P.O. Box 9177948974, Mashhad, Iran
e-mail: pakizeh@um.ac.ir

M. Namvar-Mahboub
Department of Chemical Engineering, University of Gonabad, Gonabad, Iran

Introduction

Decline of water quality and sources have become a global problem whereas access to safe and clean drinking water is essential for human life. Accordingly, World Health Organization (WHO) has specified permissible level of wastewater contaminant for different industries. One of the most widespread water contaminants are nitrate compounds which are inserted into the environment through intensive agriculture. WHO identified maximum allowable concentration of 50 mg/L for nitrate compound disposal (Ghaee et al. 2017). Several attempts have been made to remove nitrate from water due to its adverse effects on human health (Breida et al. 2018).

Up to now, different methods have been introduced for nitrate removal including biological denitrification, ion exchange, electrodialysis, adsorption, and nanofiltration (NF) (Ghaee et al. 2017; Wang and Chu 2016; Xiong et al. 2009; Yan et al. 2016; Bi et al. 2011). Among the abovementioned methods, NF process has

Published online: 14 May 2019

recently attracted great interests for its advantages such as simultaneous removal of pesticides, microorganisms, and decline of water hardness (Ghaee et al. 2017). In the case of NF process, some nitrate removal studies have done using commercial NF membranes. For instance, Kim et al. (2007) studied the separation performance of NF membrane and three different types of reverse osmosis (RO) membranes for nitrate removal. Their results showed that the rejection of RO membranes was higher than the NF membrane. Garcia et al. (2006) investigated NF membrane performance at different nitrate concentrations and different transmembrane pressures and their effect on the nitrate removal. Santafé-Moros and Gozálvez-Zafrilla (2010) used NF membrane for nitrate removal and maximum rejection of 70% was obtained.

Performance of NF membrane can be adjusted by altering its material and/or microscopic structure. Polymeric membranes are the most popular membranes which can be used for NF process. The choice of polymer plays an important role in the structure, performance, and durability of resultant membranes. PVDF as high thermal, mechanical, and chemical stable polymer has received attention to apply for membrane preparation. Anyhow, high hydrophobic nature and low surface energy of PVDF lead to formation of less water permeable membrane which is highly prone to fouling. Accordingly, many methods including surface modification, doping hydrophilic polymers, and nano-inorganic filler embedding into casting solutions have been conducted to improve the properties of PVDF membranes. In the case of nanoparticles blending method, inorganic particles, such as ZrO_2, Al_2O_3, TiO_2, and SiO_2, have been employed to modify PVDF membranes. Recently, nanomaterials, particularly the nanotubular-structured materials, have attracted attentions because of their high specific surface area and high ratio of length to diameter (Liu et al. 2011).

SNTs as one of the nanotubular materials depict potential applications for decomposition of pollutants and organic molecular separation (Jung et al. 2010). There are various methods introduced by researchers to synthesize of SNTs. Yin et al. (2010) was studied on the synthesis of SNTs using multi-walled carbon nanotube (MWCNT) as a template. The synthesized nanotube had a thickness of about 10 nm in the outer walls. This method was a facile technique for the synthesis of porous hollow SNTs. Lin and Shen (2010) studied the synthesis of SNTs through chlorosilanization of single-wall carbon nanotubes and subsequently high-temperature calcination and their resultant SNTs had the diameter at the range of 5–23 nm. Zhang et al. (2012) applied anodic alumina (PAA) and polycarbonate membranes as hard template to synthesize SNTs with orientation-controlled mesopores by interfacial growth. Kaifeng et al. (2015) studied on preparation and characterization of single-crystal SNTs. The inner diameter was at the range of the 40–60 nm and the length about 500 nm. Ananth et al. (2015) introduced a novel modified sol-gel template method to prepare SNTs on anodic alumina membrane in the presence of phosphoric acid. The nanotube had diameters in the range of 220–280 nm and the thickness of about 70–90 nm.

Regarding its superior properties, SNTs can be applied as modifier to improve separation properties of PVDF membranes. They provide many accessible active sites to be compatible with the PVDF polymer along the direction of polymer chains, particularly in their length direction (Liu et al. 2011). Additionally, as reported by Zhang et al. (2014), SNTs can improve the hydrophilicity of PVDF membrane. To the best of our knowledge, there has been no report on the application of a PVDF/SNTs membrane for nitrate removal from water.

Accordingly, the current work focused on the preparation and characterization of efficient PVDF/SNTs membrane. The study was conducted in two steps; at first, SNTs were synthesized by hydrothermal method. Then, as-prepared SNTs were incorporated into PVDF matrix to prepare nanocomposite membrane for nitrate removal. The effect of SNTs dosage on the physicochemical properties, structure, and separation performance of PVDF/SNTs membranes was also investigated. The as-prepared SNTs and membranes were characterized by ATR-FTIR, SEM, TEM, SAXS, and contact angle.

Materials and methods

Chemicals

PVDF ($\overline{Mw}$.: 440000 g/gmol) was purchased from Arkema Co. as polymer for preparation of the membrane. N-Methyl-2-pyrrolidone (NMP; Merck) was used as solvent. Cetrimonium bromide (CTAB; Mw: 364.45 g/mol), $NH_3.H_2O$ (25%) solution, and carbon nanotubes (CNTs) as a template were used to synthesize SNTs; tetraethyl orthosilicate (TEOS, 99%) were obtained from Merck company. CNTs with outside

diameter of 5–15 nm and inside diameter of 3–5 nm were applied as soft template. $Mg(NO_3)_2$ salt with analytical grade (Merck) was used to prepare initial concentration of nitrate solution. All solutions were prepared using deionized water (DI).

Synthesis of SNTs

SNTs were synthesized according to procedure reported by Wang et al. (2009). In brief, 2.4 g of CTAB was dissolved in deionized water (DI). Then 14 mL of NH_3. H_2O was added into solution and stirred for 15 min followed by addition of 1.2 g CNTs. The resultant dispersion was stirred for 3 h at room temperature. After that, TEOS (99%) was slowly added into the solution and further stirring for 2 h. The homogenous solution was placed into an autoclave at the temperature of 100 °C for 72 h. Finally, sample was centrifugal washed, dried at 50 °C, and then calcined at 700 °C to obtain white powder of SNTs. Calcination is the final step of SNTs synthesis procedure where template is removed.

Preparation of PVDF/SNTs membrane

The mixed matrix membranes were prepared via phase inversion method. The schematic of preparation procedure is presented in Fig. 1.

Initially, certain amount of as-synthesized SNTs (0–6 wt.%) were added to NMP and sonicated for 30 min. Then PVDF was gradually added into solution and dissolved with stirring to obtain 20 wt.% of polymer. Next, the solution was kept at room temperature for removal of air bubbles. The homogeneous solution was cast on a glass plate using a casting bar (Neurte 2281205). After evaporation for a certain time, the resultant film was immersed in water bath to form asymmetric membrane. The membrane was kept in the coagulation bath for 24 h to remove most of the solvent. As-prepared PVDF/SNTs membranes were nominated according to SNTs dosage (Table 1).

Characterization

SEM and TEM

The morphologies of the as-synthesized SNTs and PVDF/SNTs membranes were observed by SEM (LED 1450 VP, Germany) at 20 kV. To further investigate structure of SNTs, TEM (CM120, Philips, Holland) at 100 kV was used. For SNTs, samples were sonicated in ethanol, drop-casted on a carbon-coated copper grid, and ethanol was allowed to evaporate. For cross-sectional images of mixed matrix membranes, samples were freeze-fractured in liquid nitrogen. All samples were coated with gold-palladium to provide high electrical conductivity and high-quality images. Energy dispersive spectrometer (EDS) was used to analyze the composition of the prepared samples.

FTIR and ATR-IR

The functional groups of SNTs were recorded on a spectroscope (Thermo Nicolet Avatar 370) in the range of 690 to 4000 cm^{-1}. In the case of PVDF/SNTs membranes, ATR-FTIR was applied using Thermo Nicolet Nexus 100 ATR-IR coupled to a ZnSe crystal at a 45° operating angle.

SAXS

SAXS patterns of as-synthesized SNTs were conducted using XPERT-PRO system equipped with Cu Kα radiation source (rotating anode operated at 40 kV, 40 mA). Sample was placed in the hole of an aluminum sample holder and secured with a Kapton tape.

Contact angle

The hydrophilicity of the membranes was determined via contact angle measurement. The sessile drop contact angle method of DI water was applied using OCA15 plus a goniometer (Data Physics; USA). The data was reported as the mean value of samples, which were taken as averages of the left and right plateau contact angles at three sites for each sample (Medhat Bojnourd and Pakizeh 2018).

Membrane performance experiments

The performance of as-prepared membranes was investigated through nitrate removal from aqueous solution. Experiments were carried out at 50, 100, and 150 mg/L of nitrate concentration using the cross-flow module with effective membrane area of 0.00196 m^2. Operating condition was set at temperature of 23 °C and pressure of 7 bar. Performance parameters were evaluated in terms of PWP, PWF

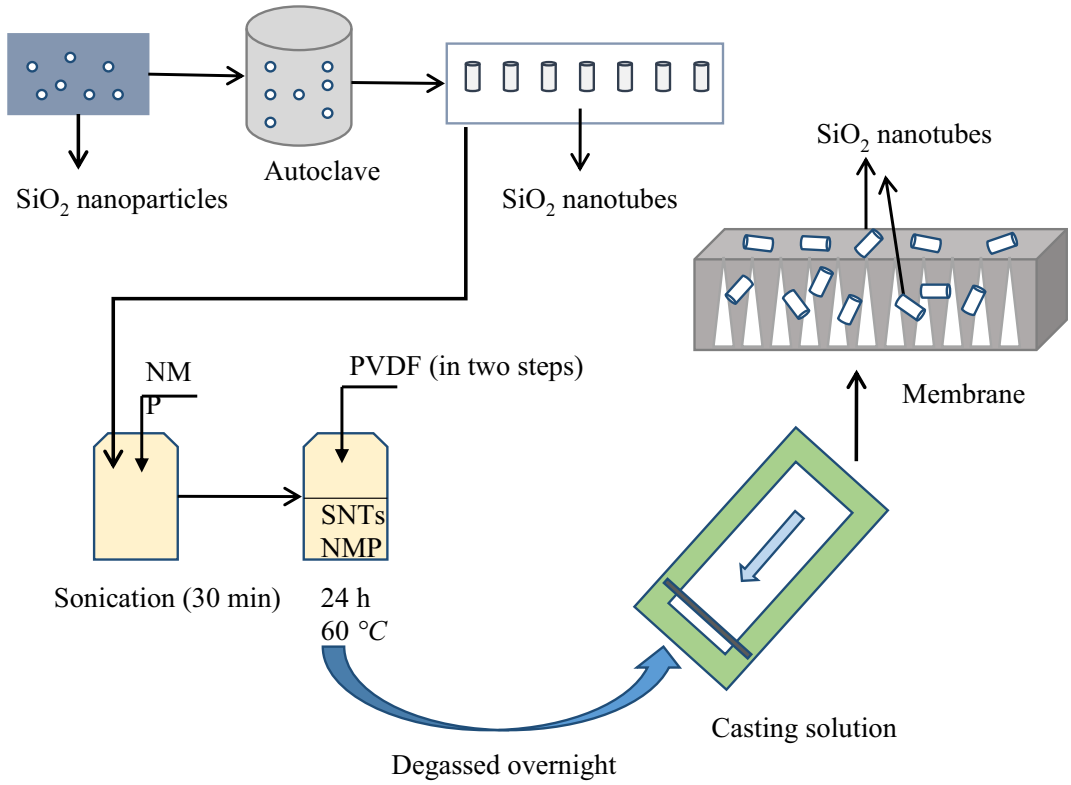

Fig. 1 Schematic of PVDF/SNTs preparation process

(pure water flux), and nitrate rejection. The PWP and PWF were calculated by the following equation:

$$\mathrm{PWP} = \frac{V}{A.t.\Delta p} \tag{1}$$

$$\mathrm{PWF} = \frac{V}{A.t} \tag{2}$$

Where V (L) is the permeate volume, A (m^2) is the effective membrane area, t (h) is the permeate collection time and Δp (bar) is the pressure difference.

Table 1 Weight percentage composition of the as-synthesized membranes

Membrane	Composition (PVDF/SNTs/NMP)
PVDF	20/0/80
PVDF/SNTs-2	20/2/78
PVDF/SNTs-4	20/4/76
PVDF/SNTs-6	20/6/74

The rejection, R (%), is calculated by the following equation:

$$R = \left(1 - \frac{C_p}{C_f}\right) \times 100 \tag{3}$$

Where C_f is the nitrate concentration in the feed solution (mg/L) and C_p is the nitrate concentration in the permeate (mg/L). The concentrations of nitrate ion were determined from its UV absorbance values at 196 nm, measured using a UV–visible spectrophotometer (Optizen POP; Mecasys; South Korea).

Table 2 The different types of fouling

Fouling type	Equation	Equation no.
Reversible fouling	$\frac{J_2 - J_0}{J_1}$	(5)
Irreversible fouling	$\frac{J_1 - J_2}{J_1}$	(6)
Total fouling	$\frac{J_1 - J_0}{J_1}$	(7)

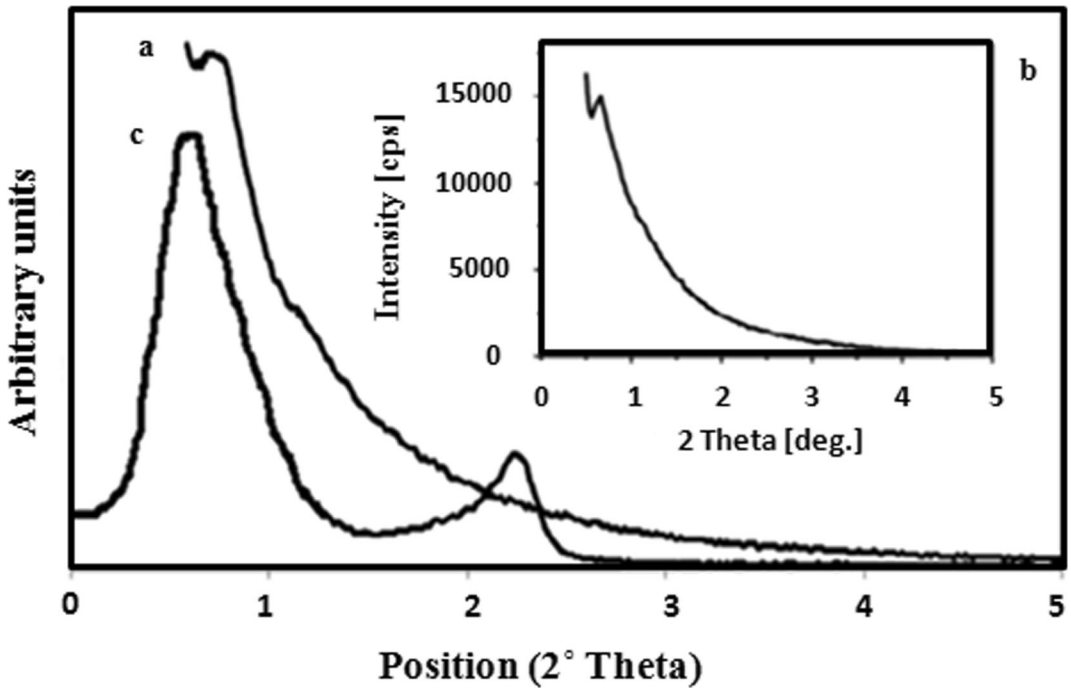

Fig. 2 SAXS pattern of **a** SNTs calcined at 700 °C, **b** Zhang et al., and **c** as-synthesized silica nanoparticles

The antifouling performance of the membranes was calculated by comparing the PWF before and after the nitrate solution filtration. The process was conducted as follows. The steady-state PWF before filtration was measured as J_1. Then the nitrate solution was filtered through the membrane, and the steady-state permeate flux was considered as J_0. After filtration of the nitrate solution, the membrane was washed with water for 10 min. Finally, the steady-state PWF after filtration was measured as J_2. The flux declines of different types of fouling were calculated based on equations shown in Table 2. Additionally, fouling resistance ability of as-prepared membranes was determined using FRR (flux recovery ratio) (Eq. 4) (Golpour and Pakizeh 2017):

$$\mathrm{FRR}(\%) = \frac{J_2}{J_1} \times 100 \tag{4}$$

Results and discussion

SAXS of SNTs

The SAXS patterns of the as-synthesized SNTs after calcination and as-synthesized silica nanoparticles are displayed in Fig. 2. The XRD pattern of SNTs, which is reported by Zhang et al. (2012), was also presented in this figure. As stated by Zhang et al. (2012), hydrothermal treatment shows no individual effect on structure of SNTs. Also, the presence of only one peak confirms the formation of pure SNTs. Moreover, by comparing the XRD analysis of as-synthesized silica particles and SNTs, it was found that the tubular structure of the SNTs was well formed.

TEM and SEM analysis of SNTs

Figure 3 gives TEM and SEM images of the as-synthesized SNTs after calcinations at 700 °C. As can be observed, SNTs have light center with dark edges which confirmed formation of nanotube structure (Wang et al. 2001). It can also be found (Fig. 3a) that the outside diameter of SNTs is less than 100 nm (Zhang et al. 2012; Kaifeng et al. 2015). The tubular morphology of as-synthesized SNTs is also confirmed by SEM images (Fig. 3b). The SNTs were observed with diameters of 80–100 nm.

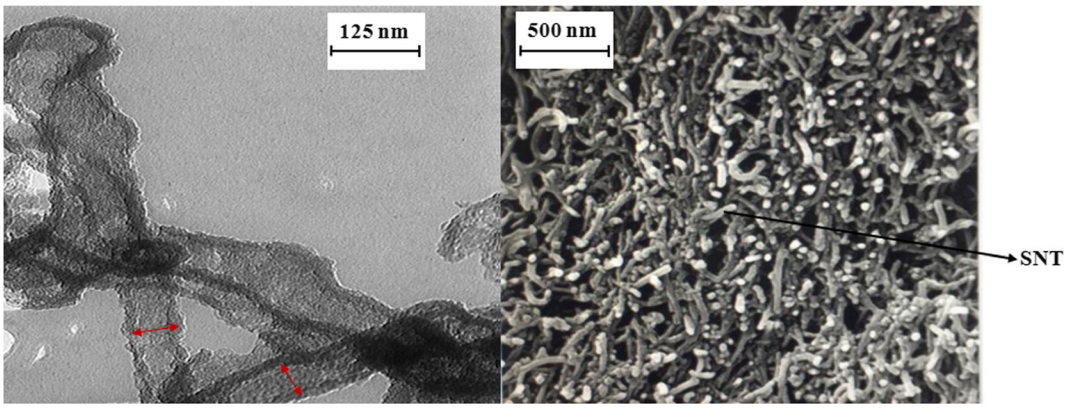

Fig. 3 **a** TEM and **b** SEM images of the as-synthesized SNTs

SEM analysis of PVDF/SNTs membranes

Surface morphology of as-prepared pure PVDF and mixed matrix membranes are presented in Fig. 4. From this figure, it can be found that the incorporation of SNTs into polymer matrix increases surface pores of resultant membranes. By increment of SNTs dosage from 0 to 4%, amount of SNTs on top surface of PVDF/SNTs membrane increases. However, no significant agglomeration of nanotubes is observed. Further increase of SNTs to 6% leads to reduction of surface pore of PVDF/SNTs-6 when compared with that one of PVDF/SNTs-4. In addition, SNTs agglomerate significantly on top surface of PVDF/SNTs-6. The mentioned trend is consistent with cross-sectional structure of as-prepared membranes. Moreover, EDS analysis for the recognition of presence of SNTs on the surface of the membranes (PVDF/SNTs-4) is displayed in Fig. 4. As can be seen, Si and O peaks are presented on EDS spectra which are belonged to SNTs. Additionally, it can be found from high-magnification SEM image that SNTs are well-distributed on PVDF/SNTs-4 surface.

The SEM cross-sectional view of the PVDF and PVDF/SNTs membranes are shown in Fig. 5. In all cases, images are presented at two magnifications. For pure PVDF membrane, both finger-like macropores and sponge-like structure can be observed. By incorporation of SNTs into polymer matrix, the morphology of PVDF membranes is changed. In the case of PVDF/SNTs-2, finger-like pores have been elongated across the membrane and more open structure can be observed when compared with pure PVDF membrane. By increasing SNTs dosage from 2 to 4%, finger-like pores tend to become disordered and portion of sponge-like structure decreases. Finally, for PVDF/SNTs-6, more dense structure can be seen among all PVDF/SNTs samples.

As stated before, structure of PVDF/SNTs membrane alters by increment of filler dosage. The abovementioned trend can be explained via two contradictory effects of nanofiller. SNTs increase solvent-nonsolvent exchange rate due to its porous structure and hydrophilic nature. Thus, it is expected that instantaneous demixing occurs during immersion step (Yin and Deng 2015). On the other hand, the presence of SNTs in casting solution decreases solvent concentration and plays a hindrance role. The hindrance effect leads to delayed demixing and as a consequence less porous structure (Kiani et al. 2018). It seems that at low concentration of SNTs, its role as accelerator of solvent-nonsolvent exchange is the dominant effect. While at SNTs dosage of 6%, its hindrance effect during immersion step overcomes effect of hydrophilic and porous structure of SNTs.

Cross-sectional view of the PVDF/SNTs-4 and its EDS spectrum was obtained at high magnification to probe the presence of SNTs along membrane structure (Fig. 6). As can be seen, characteristic peak of F and C belonged to PVDF chains and characteristic peak of Si and O are attributed to SNTs.

According to EDS spectra from both surface and cross-section of as-prepared PVDF/SNTs membrane, it can be stated that SNTs are presented on the top surface and through the structure of PVDF membrane.

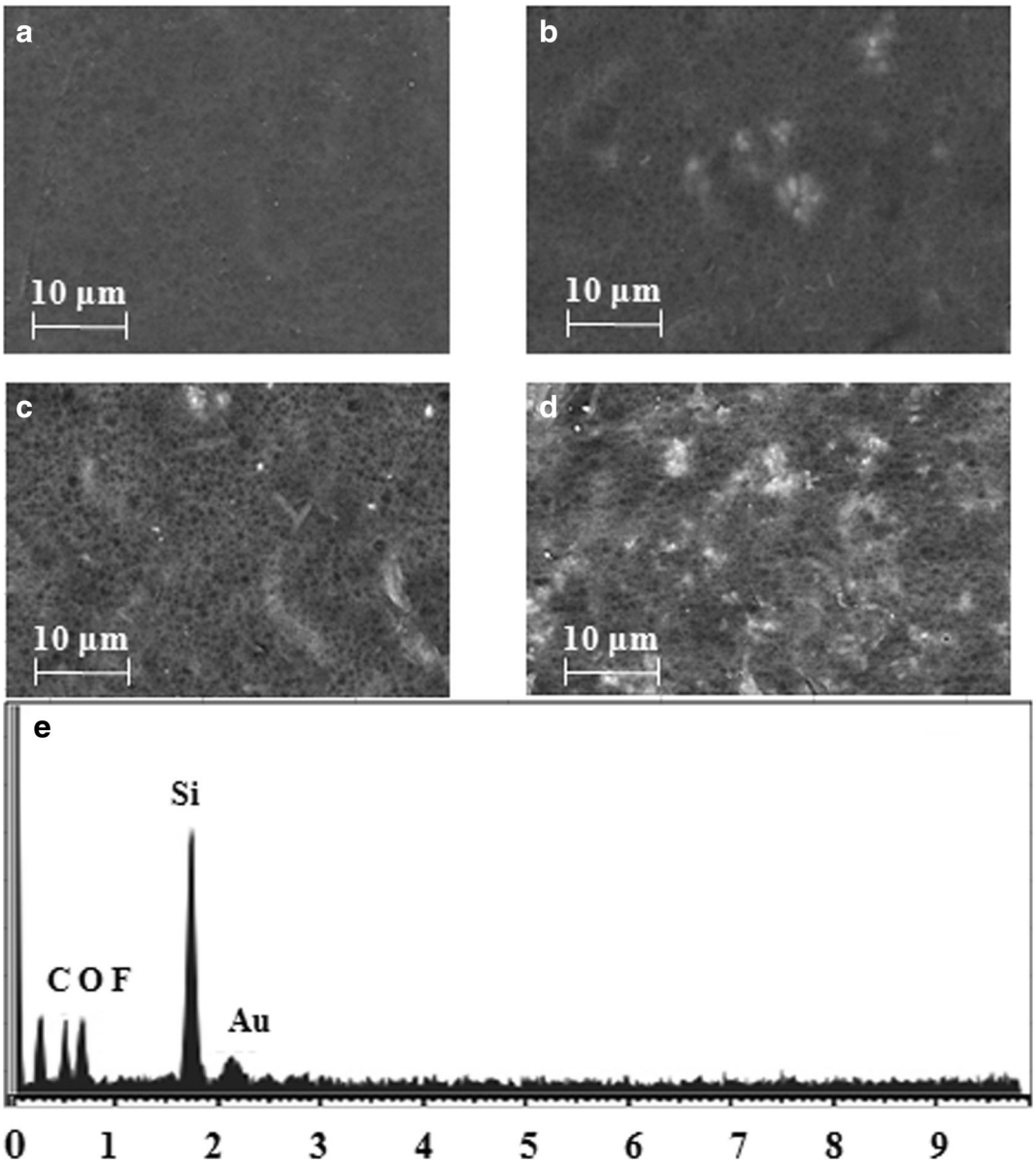

Fig. 4 Surface SEM images of membranes: **a** PVDF, **b** PVDF/SNTs-2, **c** PVDF/SNTs-4, **d** PVDF/SNTs-6, and **e** EDS of PVDF/SNTs-4

Chemical structure studies

FTIR of SNTs

FTIR was used to determine the functional groups of the as-synthesized SNTs and SNTs spectra are shown in Fig. 7. As illustrated in the figure, the vibration mode of O-Si-O bending can be observed at 463 cm^{-1}. The band at 811 cm^{-1} is assigned to the vibration mode of Si-O-Si bond. The characteristic absorption band of Si-O appears at 1085 cm^{-1}. The band at 3490 cm^{-1} indicates the presence of bending modes of hydroxyl group (OH). According to the abovementioned results on the FTIR spectra of SNTs, one can conclude that chemical structure of SNTs is successfully formed. Moreover, the results show that calcination at 700 °C removes other materials such as soft template (Ananth et al. 2015).

ATR of the as-prepared membranes

ATR-FTIR analysis was performed to investigate the presence of SNTs and its effect on chemical

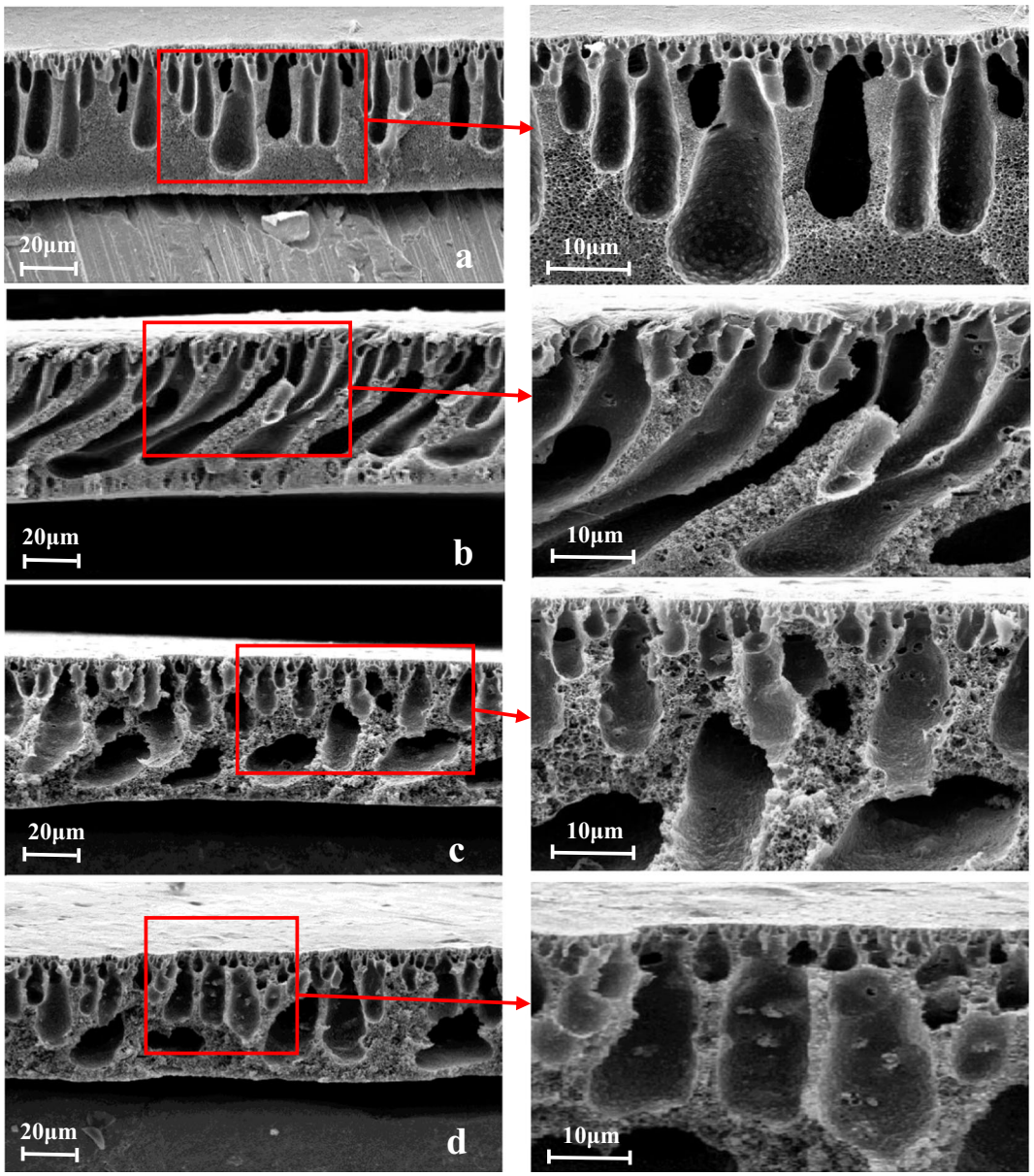

Fig. 5 SEM images of the **a** PVDF membrane, **b** PVDF/SNTS-2 membrane, **c** PVDF/SNTS-4 membrane, and **d** PVDF/SNTS-6 membrane

structure of as-prepared membranes. The results of ATR spectrum of the pure PVDF and PVDF/SNTs membranes are also shown in Fig. 7. As it is illustrated, for pure PVDF membrane, C-F stretch of PVDF chain is observed at 1191 cm^{-1}. The peak at 1380 cm^{-1} is shown the stretching vibration of C–H. The absorption bands at 1070–1236 cm^{-1} are characteristic bands of CF_2 functional group of PVDF (Lu et al. 2017). The peak at 1403 cm^{-1} is shown the vibration mode of -CH_2 (Davenport et al. 2016; Bai et al. 2012). It should also be notified that transition bands below 1000 cm^{-1} is inherent to PVDF phases (Wang et al. 2015).

In the case of PVDF/SNTs membranes, all characteristic bands of PVDF chains can be observed. The stretching peak of OH is appeared at 3420 cm^{-1} due to the presence of SNTs in polymer matrix. Additionally, main characteristic band of SNTs (Si-O-Si) is overlapped with the corresponded characteristic bands of PVDF chains. Furthermore, the

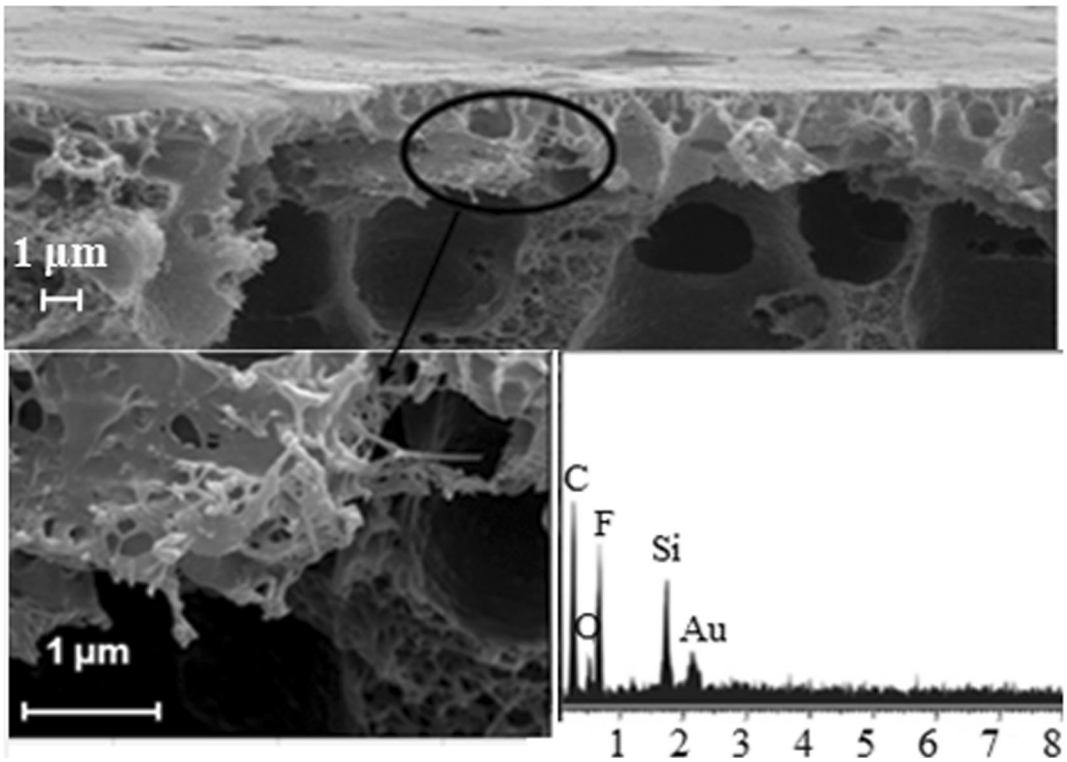

Fig. 6 High magnification of cross-sectional SEM image and EDS of PVDF/SNTs-4

band at 1191 cm^{-1} for pure PVDF is changed to 1179 cm^{-1} for PVDF/SNTs membrane as a result of polymer-SNTs interactions in the case of hydrogen bonding (Wang et al. 2012).

The effect of SNTs on the crystallinity of PVDF is also examined by ATR-FTIR spectra. PVDF membrane contains different crystalline phase which can be detected by FTIR spectra. In this case, wavenumber of about 760 and 840 cm^{-1} is related to the α and β crystalline phases of PVDF (Lai et al. 2014). As illustrated in Fig. 7, by addition of SNTs into polymer matrix, the band intensity of α phase is slightly decreased. Moreover, the intensity remains approximately unchanged for β phase band due to presence of SNTs. This behavior can be explained according to the rate of precipitation during phase inversion process. As stated before, by incorporation of SNTs, the rate of solvent-nonsolvent exchange increases which prevents SNTs to act as nucleating agent for more crystallization. The same trend was observed by Xiong et al. (2012) where SNTs was inserted into PVDF matrix.

Contact angle measurements

The contact angle values were measured to determine the surface hydrophilicity of the as-prepared membranes. The average contact angle values of pure PVDF membrane and mixed matrix membranes are presented in Table 3. As it is reported in Table 3, contact angle value decreases from 83.8° for pure PVDF to 68° for PVDF/SNTs-2. The considerable reduction of contact angle may be attributed to the presence of hydrophilic SNTs on top surface of PVDF/SNTs membrane. Indeed, SNTs can change hydrophilic property and surface structure of PVDF membrane (Liu et al. 2011). It is expected that by increasing SNTs dosage from 2 to 4%, surface hydrophilicity increases. More SNTs dosage as hydrophilic filler leads to formation of larger surface pores which can assess the reduction of contact angle values. Interestingly, at higher dosage of SNTs (6%), very slight enhancement of surface hydrophilicity is observed which may be due to SNTs agglomeration and as a consequence, decrease their specific surface area. In summary, the best hydrophilic property is obtained for PVDF/SNTs-4 and PVDF/SNTs-6.

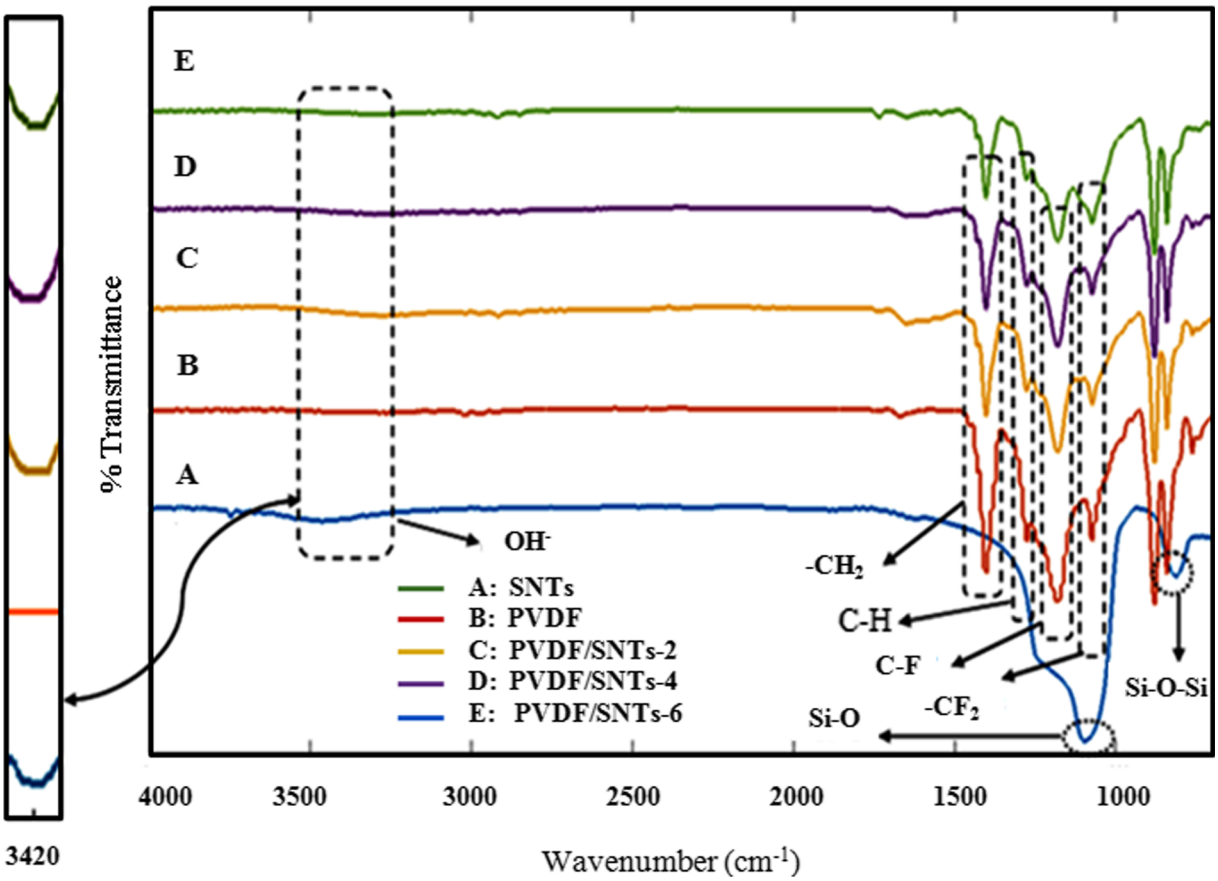

Fig. 7 ATR-FTIR spectra for the SNTs, PVDF membrane, PVDF/SNTs-2 membrane, PVDF/SNTs-4 membrane, and PVDF/SNTs-6 membrane

Membrane permeation properties

PWP and nitrate rejection performance

The PWP and the nitrate rejection of the as-prepared membranes were determined at 7 bar operating pressure. Figure 8 presents the PWP of as-prepared membranes as a function of time. For all samples, PWP decreases with respect to time due to membrane compaction (Liu et al. 2011). To study the effect of SNTs dosage on PWP of mixed matrix membranes, steady-state values of PWP is considered. As shown in Fig. 8, the PWP of the membranes increase when SNTs are inserted into PVDF matrix. By increasing SNTs content, PWP first increases from 6.68 to 11.58 L/(m^2.h.bar) for PVDF and PVDF/SNTs-4, respectively, and then decreases to 10.25 L/(m^2.h.bar) for PVDF/SNTs-6. Therefore, it can be stated that optimal permeability is achieved at 4% of SNTs. The observed trend can be explained according to morphology and hydrophilicity of membranes and SNTs structure. As stated by contact angle results, the hydrophilicity of the membranes is improved by increasing the amount of SNTs. More hydrophilic surface causes higher water permeability. In addition, more open structure of as-prepared PVDF/SNTs improves PWP (Ali 2016). Besides, high ratio of length to diameter of SNTs causes the desirable potential application in improving properties of PVDF membranes. Regarding SNTs porous structure, this filler provides additional pathway for water molecule transportation across the PVDF

Table 3 Contact angle values of the as-prepared membranes

Membranes	Contact angle (°)
PVDF	83.8 ± 0.4
PVDF/SNTs-2	68.0 ± 0.5
PVDF/SNTs-4	58.0 ± 1.2
PVDF/SNTs-6	60.0 ± 0.7

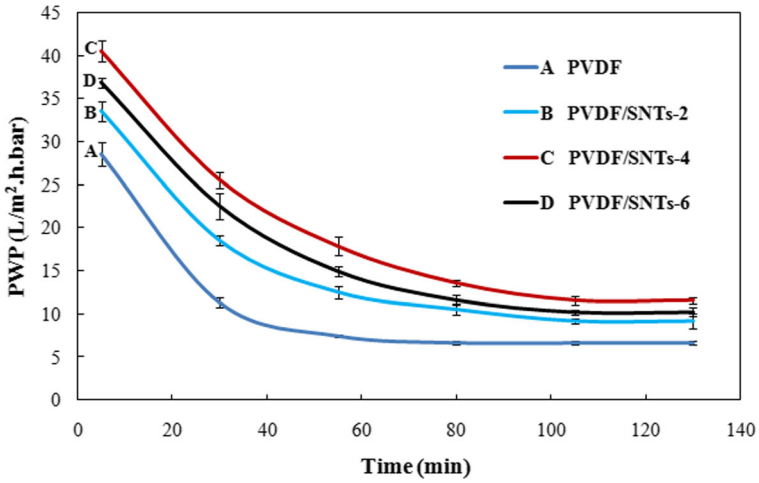

Fig. 8 PWP of the membranes ($\Delta p = 7$ bar and $T = 23$ °C)

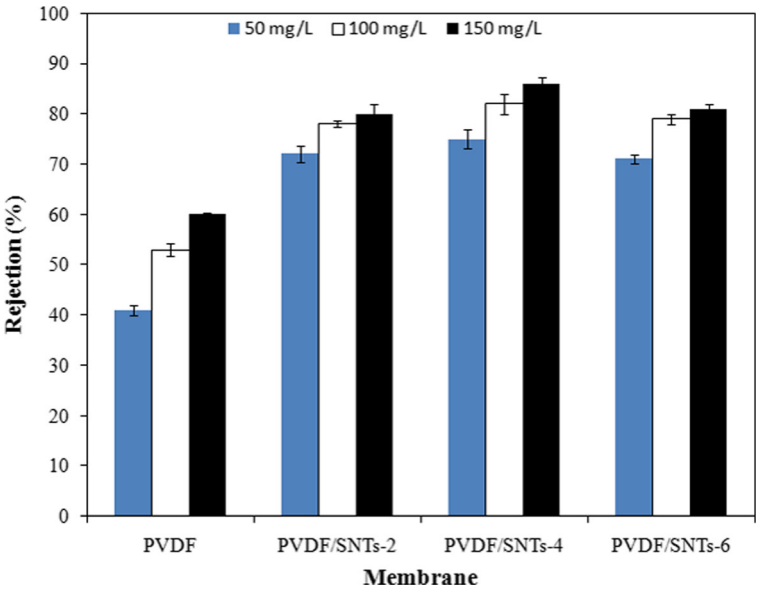

Fig. 9 The nitrate rejection of PVDF, PVDF/SNTs-2, PVDF/SNTs-4, and PVDF/SNTs-6 membranes ($C_f = 50$, 100, 150 mg/L; $\Delta p = 7$ bar; and $T = 23$ °C)

membrane. All mentioned effects assess PWP improvement of mixed matrix membranes. In the case of PVDF/SNTs-6 membrane, PWP reduction is a result of SNTs agglomeration and reduction of membrane pore size.

Figure 9 shows the results of the nitrate rejection for pure PVDF and PVDF/SNTs membranes at different nitrate concentration (50, 100, and 150 mg/L). As can be seen, by increasing solute concentration from 50 to 150 mg/L, rejection increases for all samples. By

Table 4 The flux recovery ratio for PVDF and PVDF/SNTs-4 membranes at 7 bar

Membrane	Flux (L/m^2.h)			Decline flux (%)			FRR (%)
	J_1	J_0	J_2	Reversible	Irreversible	Total	
PVDF	24.5	6.68	15.75	37	35.71	72.7	64.3
PVDF/SNTs-4	49.28	24.63	43.85	39	11.01	50	88.9

Table 5 A comparison between the previous studies and this study for nitrate removal

Membrane type	Rejection (%)	Permeability (L/(m^2.h.bar))	Ref.
Nanofiltration, PA-zeolite/PSf membrane	85	3	(Ghaee et al. 2017)
Nanofiltration (NTR729HF), RO (CPA2, LFC1, and ESPA1)	60–90	7.6	(Wang and Chu 2016)
Nanofiltration, (OPMN-P)	88	7.2	(Yan et al. 2016)
Nanofiltration, SU-61	70	NA*	(Bi et al. 2011)
Nanofiltration, UTC-20	88	NA	(Kang et al. 2009)
Nanofiltration, NF270	90	8.89	(Santafé-Moros et al. 2005)
Nanofiltration, PVDF/SNTs membrane	86	11.58	This study

*Not available

incrementing feed concentration, more hydrated nitrate may be formed and nitrate rejection increases as a result of steric hindrance effect (Paugam et al. 2002).

For fixed value of feed concentration, the presence of SNTs in PVDF matrix improves nitrate rejection. Increasing SNTs dosage from 0 to 4% increases nitrate rejection due to PWP improvement. Indeed, SNTs as hydrophilic filler affect water molecule transport rate more than nitrate ions and therefore enhance rejection values. The same trend of nitrate rejection value was observed by Ghaee et al. (2017) for nanocomposite membranes. The resultant PWP and nitrate rejection reveal that the optimum amount of SNTs is 4% in the range of 0 to 6%.

Antifouling properties of the NF membrane

The antifouling performance of PVDF/SNTs-4 as optimum membrane was studied through nitrate removal of 150 mg/L feed solution at 7 bar and 23 °C. The obtained results in terms of J_1, J_2, flux decline, and FRR values were compared with that one of pure PVDF membrane. Fouling parameters of both membranes are presented in Table 4. As illustrated, SNTs enhance antifouling of PVDF membrane by about 38%. Certainly, hydrophilic nature of SNTs and their impact on surface hydrophilicity of PVDF/SNTs membrane play a crucial role in antifouling property of resultant PVDF/SNTs membrane.

Although it is difficult to find the same conditions to study on the experiments, here, it has been tried to compare the previous studies on nitrate removal and the present work. The performance parameters (rejection and permeability) of each study are summarized in Table 5. As can be seen, the performance of optimum PVDF/SNTs membrane is comparable with NF270 commercial membrane. Additionally, PVDF/SNTs show better performance than applied commercial membranes for nitrate removal.

Conclusions

In this study, the nitrate was removed from aqueous solution using PVDF-based NF membrane. The effect of SNTs as a filler on characteristic and performance of PVDF membrane was investigated. In this regard, SNTs were successfully synthesized using hydrothermal method. The mixed matrix membranes were prepared by the incorporation of SNTs into PVDF polymer matrix via solution blending and phase inversion methods. The obtained results showed that SNTs altered the morphology of the membrane through change of the pores structure. Additionally, EDS spectra confirmed the presence of SNTs through and on the top surface of as-prepared membranes. Hydrophilicity of PVDF membrane had been considerably increased in the presence of SNTs. PWP of PVDF/SNTs-4 increased by about 73% in comparison with that one of pure PVDF membrane. Additionally, the maximum rejection of 86%was obtained for PVDF/SNTs-4. Regarding the performance results, 4% of SNTs is the optimum filler dosage. It was also found that PVDF/SNTs had superior antifouling resistance when compared with pure PVDF membrane.

Funding information This study received financial support from Iran Nanotechnology Initiative Council.

Compliance with ethical standards

Conflict of interest The authors declare that they have no conflict of interest.

References

Ali MEA (2016) Thin film composite membranes incorporated with graphene oxide nanosheets; preparation and performance in water desalination. Sustainable Vital Technologies in Engineering & Informatics, pp 1–22

Ananth KP, Jose SP, Mangalaraj D, Nathanael AJ, Ballamurugan AM, Oh TH (2015) A novel modified sol-gel template synthesis of high aspect ratio silica nanotubes in the presence of phosphoric acid. J Nanopart Res 35:27–38. https://doi.org/10.4028/www.scientific.net/JNanoR.35.27

Bai H, Wang X, Zhou Y, Zhang L (2012) Preparation and characterization of poly (vinylidene fluoride) composite membranes blended with nano-crystalline cellulose. Prog Nat Sci Mater Int 22(3):250–257. https://doi.org/10.1016/j.pnsc.2012.04.011

Bi J, Peng C, Xu H, Ahmed AS (2011) Removal of nitrate from groundwater using the technology of electrodialysis and electrodeionization. J Desalination Water Treat 34(1–3): 394–401. https://doi.org/10.5004/dwt.2011.2891

Breida M, Younssi SA, Bouazizi A, Achiou B, Ouammou M, El Rhazi M (2018) Nitrate removal from aqueous solutions by γ-Al_2O_3 ultrafiltration membranes. Heliyon 4(1):e00498. https://doi.org/10.1016/j.heliyon.2017.e00498

Davenport DM, Gui M, Ormsbee LR, Bhattacharyya D (2016) Development of PVDF membrane nanocomposites via various functionalization approaches for environmental applications. Polymers 8(2):32. https://doi.org/10.3390/polym8020032

Garcia F, Ciceron D, Saboni A, Alexandrova S (2006) Nitrate ions elimination from drinking water by nanofiltration, membrane choice. Sep Purif Technol 52(1):196–200. https://doi.org/10.1016/j.seppur.2006.03.023

Ghaee A, Zerafat M, Askari P, Sabbaghi S, Sadatnia B (2017) Fabrication of polyamide thin-film nanocomposite membranes with enhanced surface charge for nitrate ion removal from water resources. Environ Technol 38(6):772–781. https://doi.org/10.1080/09593330.2016.1231223

Golpour M, Pakizeh M (2017) Development of a new nanofiltration membrane for removal of kinetic hydrate inhibitor from water. Sep Purif Technol 183:237–248. https://doi.org/10.1016/j.seppur.2017.04.011

Jung JH, Park M, Shinkai S (2010) Fabrication of silica nanotubes by using self-assembled gels and their applications in environmental and biological fields. Chem Soc Rev 39:4286–4302. https://doi.org/10.1039/C002959A

Kaifeng Y, Song M, Gao X, Wang F, Hou C (2015) Preparation and characterization of single-crystal silica nanotubes. J Syn React Inorganic, Metal-Organic Nano-Metal Chem 45(5): 770–772. https://doi.org/10.1080/15533174.2013.843552

Kang M, Jeong TK, Hwang IH (2009) Nitrate by nanofiltrations in very small drinking water systems. World Appl Sci J 5:41–45

Kiani S, Mousavi SM, Saljoughi E, Shahtahmassebi N (2018) Preparation and characterization of modified polyphenylsulfone membranes with hydrophilic property for filtration of aqueous media. Polym Adv Technol 29(6): 1632–1648. https://doi.org/10.1002/pat.4268

Kim YH, Hwang ED, Shin W, Choi JH, Ha T, Choi S (2007) Treatments of stainless steel wastewater containing a high concentration of nitrate using reverse osmosis and nanomembranes. Desalination 202(1–3):286–292. https://doi.org/10.1016/j.desal.2005.12.066

Lai CY, Groth A, Gray S, Duke M (2014) Preparation and characterization of poly(vinylidene fluoride)/ nanoclay nanocomposite flat sheet membranes for abrasion resistance. Water Res 57:56–66. https://doi.org/10.1016/j.watres.2014.03.005

Lin T, Shen H (2010) The synthesis of silica nanotubes through chlorosilanization of single wall carbon nanotubes. Nanotechnology 21(36):365604. https://doi.org/10.1088/0957-4484/21/36/365604

Liu F, Hashim NA, Liu YT, Abed MRM, Li K (2011) Progress in the production and modification of PVDF membranes. J Membr Sci 375:1–27. https://doi.org/10.1016/j.memsci.2011.03.014

Lu X, Peng Y, Qiu H, Liu X (2017) Anti-fouling membranes by manipulating surface wet ability and their anti-fouling mechanism. Desalination 413:127–135. https://doi.org/10.1016/j.desal.2017.02.022

Medhat Bojnourd F, Pakizeh M (2018) Preparation and characterization of a PVA/PSf thin film composite membrane after incorporation of PSSMA into a selective layer and its application for pharmaceutical removal. Sep Purif Technol 192:5–14. https://doi.org/10.1016/j.seppur.2017.09.054

Paugam L, Taha S, Cabon J, Dorange G (2002) Elimination of nitrate ions in drinking waters by nanofiltration. Desalination 152: 271–274. https://doi.org/10.1016/S0011-9164(02)01073-1

Santafé-Moros A, Gozálvez-Zafrilla J (2010) Nanofiltration study of the interaction between bicarbonate and nitrate ions. Desalination 250(2):773–777. https://doi.org/10.1016/j.desal.2008.11.039

Santafé-Moros A, Gozálvez-Zafrilla J, Lora-García J (2005) Performance of commercial nanofiltration membranes in the removal of nitrate ions. Desalination 185(1–3):281–287. https://doi.org/10.1016/j.desal.2005.02.080

Wang J, Chu L (2016) Biological nitrate removal from water and wastewater by solid-phase denitrification process. Biotechnol Adv 34(6):1103–1112. https://doi.org/10.1016/j.biotechadv.2016.07.001

Wang L, Tomura S, Ohashi F, Maeda M, Suzuki M, Inukai K (2001) Synthesis of single silica nanotubes in the presence of citric acid. J Mater Chem 11(5):1465–1468. https://doi.org/10.1039/B010189N

Wang L, Shan Z, Zhang Z, Wei F, Xiao FS (2009) One-pot hydrothermal synthesis of mesostructured silica nanotube. J Colloid Interface Sci 335(2):264–267. https://doi.org/10.1016/j.jcis.2009.03.091

Wang J, Chen P, Chen L, Wang K, Deng H, Chen F (2012) Preparation and properties of poly (vinylidene fluoride) nanocomposites blended with graphene oxide coated silica hybrids. Express Polym Lett 6(4):299–307

Wang S, Liu L, Zeng Y, Zhou B, Teng K, Ma M (2015) Improving dielectric properties of poly (vinylidene fluoride) composites effects of surface functionalization of exfoliated grapheme. J Adhes Sci Technol 29(7):678–690. https://doi.org/10.1080/01694243.2014.1003497

Xiong Z, Zhao D, Pan G (2009) Rapid and controlled transformation of nitrate in water and brine by stabilized iron nanoparticles. J Nanopart Res 11(4):807–819. https://doi.org/10.1007/s11051-008-9433-9

Xiong X, Li Q, Zhang XC, Wang L, Guo ZX, Yu J (2012) Poly(vinylidene fluoride)/silica nanocomposite membranes

by electrospinning. J Appl Polym Sci 129(3):1089–1095. https://doi.org/10.1002/app.38832

Yan W, Yi W, Jinnan W, Suqian X, Liang Y, Philippe C, Wintgens T (2016) Nitrate removal from water by new polymeric adsorbent modified with amino and quaternary ammonium groups: batch and column adsorption study. J Taiwan Inst Chem Eng 66:191–199. https://doi.org/10.1016/j.jtice.2016.06.019

Yin J, Deng B (2015) Polymer-matrix nanocomposite membranes for water treatment. J Membr Sci 479:256–275. https://doi.org/10.1016/j.memsci.2014.11.019

Yin Z, Liu X, Su Z (2010) Novel fabrication of silica nanotubes using multiwalled carbon nanotubes as a template. Bull Mater Sci 33(4):351–355. https://doi.org/10.1007/s12034-010-0053-5

Zhang A, Hou K, Gu L, Dai C, Liu M, Song C, Guo X (2012) Synthesis of silica nanotubes with orientation controlled mesopores in porous membranes via interfacial growth. Chem Mater 24(6):1005–1010. https://doi.org/10.1021/cm300242n

Zhang S, Wang R, Li G, Zhang Y (2014) Treatment of wastewater containing oil using phosphorylated silica nanotubes/polyvinylidene fluoride (PSNTs/PVDF) composite membrane. Desalination 332(1):109–116. https://doi.org/10.1016/j.desal.2013.11.008

Publisher's note Springer Nature remains neutral with regard to jurisdictional claims in published maps and institutional affiliations.